Interplay between spontaneous and induced brain activity during human non-rapid eye movement sleep

Thien Thanh Dang-Vu[a,1,2,3], Maxime Bonjean[a,b,c,d,1,3], Manuel Schabus[a,e], Mélanie Boly[a], Annabelle Darsaud[a], Martin Desseilles[a], Christian Degueldre[a], Evelyne Balteau[a], Christophe Phillips[a], André Luxen[a], Terrence J. Sejnowski[b,c,d,3], and Pierre Maquet[a]

[a]Cyclotron Research Centre, University of Liège, B-4000 Liège, Belgium; [b]Howard Hughes Medical Institute, [c]The Salk Institute, and [d]Division of Biological Sciences, University of California at San Diego, La Jolla, CA 92037; and [e]Laboratory for Sleep and Consciousness Research, Department of Psychology, University of Salzburg, A-5020 Salzburg, Austria

Contributed by Terrence J. Sejnowski, August 5, 2011 (sent for review June 15, 2011)

Humans are less responsive to the surrounding environment during sleep. However, the extent to which the human brain responds to external stimuli during sleep is uncertain. We used simultaneous EEG and functional MRI to characterize brain responses to tones during wakefulness and non-rapid eye movement (NREM) sleep. Sounds during wakefulness elicited responses in the thalamus and primary auditory cortex. These responses persisted in NREM sleep, except throughout spindles, during which they became less consistent. When sounds induced a K complex, activity in the auditory cortex was enhanced and responses in distant frontal areas were elicited, similar to the stereotypical pattern associated with slow oscillations. These data show that sound processing during NREM sleep is constrained by fundamental brain oscillatory modes (slow oscillations and spindles), which result in a complex interplay between spontaneous and induced brain activity. The distortion of sensory information at the thalamic level, especially during spindles, functionally isolates the cortex from the environment and might provide unique conditions favorable for off-line memory processing.

sleep spindles | neuroimaging | fMRI | auditory perception | sleep physiology

It is commonly believed that during non-rapid eye movement (NREM) sleep, the brain is isolated from the environment, based on an increase in the sensory threshold observed in sleeping individuals, and indirectly from the inability to remember the content of external stimuli delivered during sleep (1). However, a number of studies, ranging from single unit recordings in animals (2, 3) to human EEG (4) and neuroimaging (5) experiments, demonstrate the persistence of brain responses to sensory stimulations during NREM sleep, suggesting that the brain can still process external stimuli during NREM sleep.

In fact, the transmission of sensory information during NREM sleep is thought to be selectively reduced during sleep spindles (6, 7). Sleep spindles—a hallmark of light NREM sleep [mostly stage 2 (S2) sleep]—are characterized in humans by waxing and waning 11- to 15-Hz oscillations lasting 0.5–3 s (8). They are generated by the thalamus, which acts as a pacemaker (9, 10), and result from reciprocal rhythmic interactions between reticular (nRT) and thalamo-cortical (TC) cells. Induced by a recurrent inhibition from nRT cells, postinhibitory rebound spike bursts in TC cells entrain cortical populations in spindle oscillations (11). In turn, a cortico-thalamic feedback synchronizes spindle oscillations in widespread thalamic territories (12). It has been suggested that synaptic blockade in the thalamus filters out sensory transmissions to the forebrain during sleep spindles (13). Accordingly, in humans, modifications of auditory event-related potentials (ERPs) recorded on the scalp have been interpreted as reflecting the thalamic inhibition of information processing during spindles, although direct evidence supporting this hypothesis is still lacking (14, 15).

To assess this hypothesis, we used simultaneous EEG/functional MRI (fMRI) recordings to better characterize regional cerebral response patterns to auditory stimulations administered during wakefulness and NREM sleep [stages 2–3 (S2-3)]. Our objective was to determine how pure tones are processed during NREM sleep at the thalamic and cortical levels based on the hypothesis that auditory stimulation would still induce the activation of TC circuits during NREM sleep, except when the stimulus is delivered during a spindle.

Results

Young, non-sleep-deprived, normal human volunteers were studied by using simultaneous EEG/fMRI during the first half of the night (Fig. 1). During the whole scanning session, pure tones (300 ms, 400 Hz) were delivered randomly with a 70% probability of occurrence during each scan. Epochs corresponding to steady S2-3 sleep and devoid of arousals or shifts to wakefulness were carefully selected from the complete EEG recordings. The corresponding series of consecutive fMRI scans constituted a session and were considered for further analysis (Fig. 1*B*). Tones were classified according to whether they were delivered concurrently to a spindle [tone in spindle (TS)] or not concurrently to a spindle [tone with no spindle (TN)] (Fig. 1*C*). Waking sessions before and after sleep were also selected and analyzed separately; those sessions were used to identify brain activations associated with the occurrence of tones during wakefulness (TW). The analysis of fMRI data first characterized the brain responses to TW compared with waking baseline activity. Brain responses to the two-tone categories (TS and TN) were then assessed in comparison with the baseline activity of S2-3 sleep. To take into account the effects of all identifiable neural events on blood-oxygen level-dependent (BOLD) signal during sleep, sleep spindles and slow waves were also modeled in the analysis. Spindles were identified on bandpass-filtered EEG data between 11 and 15 Hz by using an automatic detection algorithm based on an amplitude criterion (16). Slow waves were also detected in S2-3 sleep sessions and explicitly modeled as in ref. 17. Brain responses related to spindles and slow waves have already been described (17, 18) and are not reported here in detail (Fig. S1).

Author contributions: T.T.D.-V., M. Bonjean, M.S., and P.M. designed research; T.T.D.-V., M. Bonjean, M.S., M. Boly, A.D., M.D., A.L., and P.M. performed research; C.D., E.B., C.P., A.L. contributed new reagents/analytic tools; T.T.D.-V., M. Bonjean, M.S., T.J.S., and P.M. analyzed data; and T.T.D.-V., M. Bonjean, M.S., T.J.S., and P.M. wrote the paper.

The authors declare no conflict of interest.

Freely available online through the PNAS open access option.

[1]T.T.D.-V. and M. Bonjean contributed equally to this work.

[2]Present address: Center for Advanced Research in Sleep Medicine, Hôpital du Sacré-Coeur de Montréal, University of Montreal, Montreal, QC, Canada H4J 1C5.

[3]To whom correspondence may be addressed. E-mail: tt.dangvu@ulg.ac.be, bonjean@salk.edu, or terry@salk.edu.

This article contains supporting information online at www.pnas.org/lookup/suppl/doi:10.1073/pnas.1112503108/-/DCSupplemental.

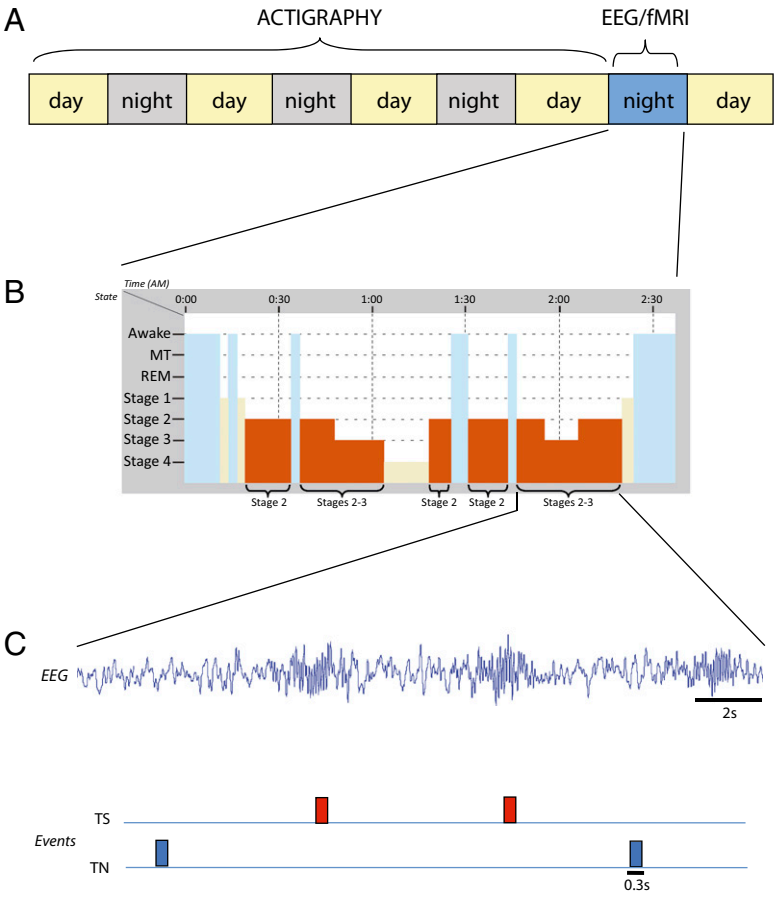

Fig. 1. Experimental protocol. (*A*) Timeline of experimental procedure. After a 4-d constant sleep schedule, volunteers were recorded with EEG/fMRI during the experimental night. (*B*) Experimental night. Sessions of continuous wakefulness (light blue) as well as S2-3 of NREM sleep (orange) with corresponding fMRI time series were selected for analysis. S1 and S4 of NREM sleep, depicted in light brown, were not used for analysis. (*C*) Events of interest included the tones categorized according to their occurrence during S2-3 within (TS, red squares) or outside (TN, blue squares) spindles.

Responses to sounds corresponded to systematic deviations of the BOLD signal over and above the baseline activity during NREM sleep, with the activity related to characteristic oscillations of NREM sleep being taken into consideration.

Out of the initial 19 volunteers, 13 were able to maintain stable S2-3 of NREM sleep in the scanner. One to seven sessions [mean (SD): 3.8 (1.9)] of S2-3 were selected per subject. In each subject, the total duration of all selected S2-3 sessions ranged from 14 to 53 min (mean 35). The mean (SD) number and density of detected spindles per subject were 107 (37) and 3.10 (0.3) min^{-1}, respectively. The mean (SD) number of TN and TS per subject was 534.3 (198.8) and 30 (11.2), respectively (but also see Table S2 for TN). The mean (SD) number of TW per subject was 161.3 (96.5). Corresponding ERPs were computed for TW, TN, and TS (Fig. S2).

As expected, TW induced responses in the primary auditory cortex (Heschl's transverse gyrus) and in the thalamus, in an area compatible with the medial geniculate nucleus (Fig. 2*A* and Table S1). TN were also associated with responses in the primary auditory cortex and the thalamus (Fig. 2*B* and Table S1; see also Table S2), demonstrating that sounds during NREM sleep are still processed in auditory areas. Significant additional responses were found in a set of cortical and subcortical areas, in the pons, cerebellum, middle frontal gyrus, precuneus, and posterior cingulate gyrus—all areas known to respond to auditory stimuli (5, 19, 20). In contrast, at the same statistical threshold ($P < 0.05$ corrected), no significant response to TS was found either in the thalamus or in the Heschl's gyri, but rather in a small area in the caudal aspect of the inferior colliculus (Fig. 2*C* and Table S1). We note that time modulation did not have a significant impact on responses to TS, suggesting that these effects were not likely to be confounded by habituation. Direct comparison between TN and TS (Fig. 3) confirmed that responses in the former were significantly higher than in the latter in the right Heschl's gyrus [$F(1, 12) = 4.48$; $P < 0.05$]. Likewise, exclusive masking (threshold at $P < 0.5$) confirmed that responses to TN in all previously reported areas were not significant in response to TS. However, inspection of the cortical and thalamic responses to TS (Fig. 2 *D* and *E*, red) revealed that they were not only smaller but also more variable than responses to TN (Fig. 2 *D* and *E*, blue), explaining the absence of significant response in these areas for TS at conservative statistical thresholds.

To further characterize the regional brain responses to tones presented during NREM sleep in the absence of spindles, we divided TN into two classes according to whether TN was followed (TNK) or not followed (TN0) by an induced K complex. The mean number of TN followed by a K complex per subject was 46.23 (ranging from 20 to 182) and found in 9% of TN. Both subcategories of TN were associated with significant responses in the primary auditory cortex, thalamus, brainstem, cerebellum, and posterior cingulate gyrus (Fig. 4 *A* and *B* and Table S3). Comparing TNK and TN0, we found that tones elicited larger responses in bilateral primary auditory cortex and ventral prefrontal cortex in the presence of an induced K complex (Fig. 4*C*).

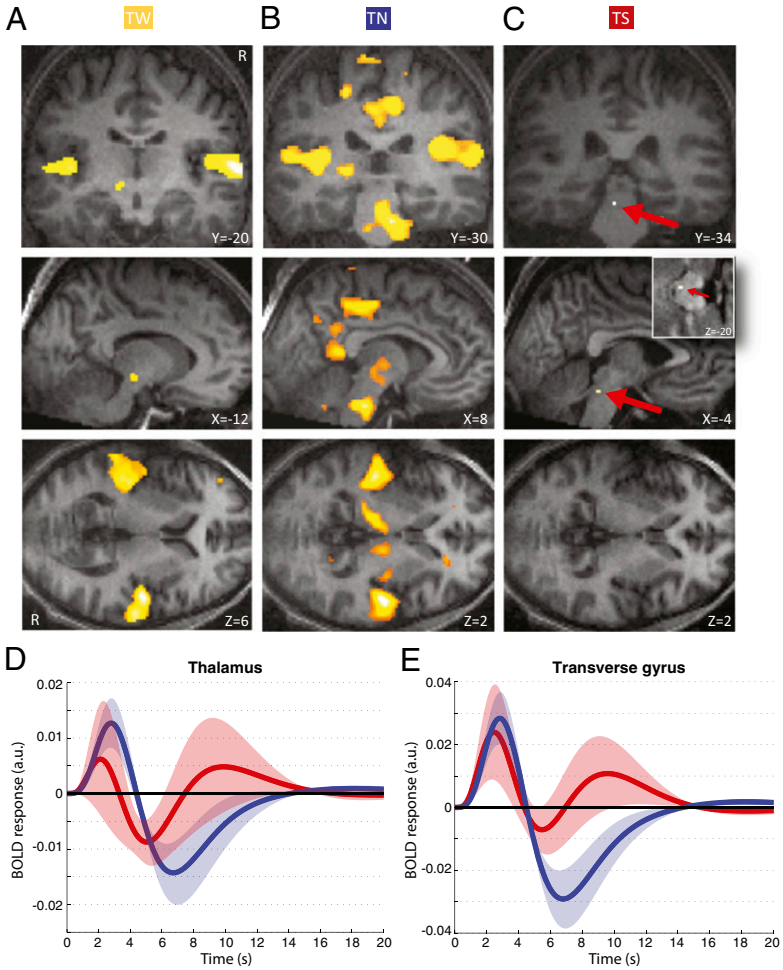

Fig. 2. Brain regions activated in relation to tones during waking (TW), NREM sleep (outside spindles; TN), and spindles (TS). (*A*) Significant responses associated with tones presented during waking. (*B*) Significant responses associated with tones presented during S2-3 NREM sleep, in the absence of ongoing spindles. These responses are located in the thalamus, primary auditory cortex, brainstem, cerebellum, middle frontal gyrus, precuneus, and posterior cingulate gyrus. The brainstem response encompasses areas compatible with the cochlear nuclear groups (peak voxel), the trapezoid bodies, and the superior olivary complex. (*C*) Significant responses associated with tones presented within spindles in S2-3 NREM sleep. In this area of the brainstem (arrow, *Inset*), neural populations that process sound are found in the nuclei of the lateral lemniscus. Functional results are displayed on an individual structural image (display at $P < 0.001$, uncorrected), at different levels of the *x*, *y*, and *z* axes as indicated for each section. (*D* and *E*) Fitted responses in the thalamus ($x = -12$, $y = -22$, $z = -6$; *D*) and the auditory cortex ($x = 58$, $y = -14$, $z = 6$; *E*) associated with sounds delivered with (red, TS) or without (blue, TN) ongoing spontaneous spindle. The curves correspond to the mean and the shaded areas to the SEM. Coordinates of the thalamus and auditory cortex were derived from the peak voxels in these areas during wakefulness (TW).

Discussion

These results show that brain responses are smaller, more variable, and less prone to be faithfully transmitted to the cortex when sounds are present during a spindle, compared with stimuli delivered outside spindles. These findings emphasize a reduction in the consistency of transmission of external inputs to the cortex during spindles, rather than an absolute obliteration of transmission as advocated by earlier work (14, 15).

The anatomical stage at which the transfer of sensory information to auditory TC pathways is hindered remains uncertain. We cannot rule out a change in sound processing in the prethalamic stages of the auditory system during NREM sleep. No clear-cut change in neural activity takes place at any of the early auditory relay structures during NREM sleep (21), but prethalamic modifications in transmission were reported in the somato-sensory system during NREM sleep, although not specifically in conjunction with spindles (22). Conversely, thalamic neurons are likely to hinder the faithful transmission of sensory input during spindles because the burst firing mode that they adopt during NREM sleep distorts the transmission of sensory inputs to the cortex in a nonlinear fashion (23, 24).

We also demonstrate a specific pattern of activation for sounds presented in the absence of spontaneous spindles. Given the different patterns observed between TW and TN (Fig. 2 *A* and *B*), it is tempting to compare and discuss their respective activations. Direct comparison between the responses to sounds during wakefulness and sleep is not warranted because of state-specific baselines. Nevertheless, responses that were selectively significant for TN and not for TW (exclusive masking; $P < 0.5$) were detected in brainstem, cerebellum, middle frontal gyrus, posterior cingulate gyrus, and precuneus. This response pattern is intriguingly similar to brain activity related to slow oscillation (17). We speculate that these responses reflect the modulation of sound-induced responses by the slow oscillation, which is a fundamental rhythm organizing neural activity during NREM sleep (25). Further analyses of sound processing during deep NREM sleep are needed to confirm this hypothesis.

Finally, we show that sounds during NREM sleep induce a larger activation of the primary auditory cortex when they are

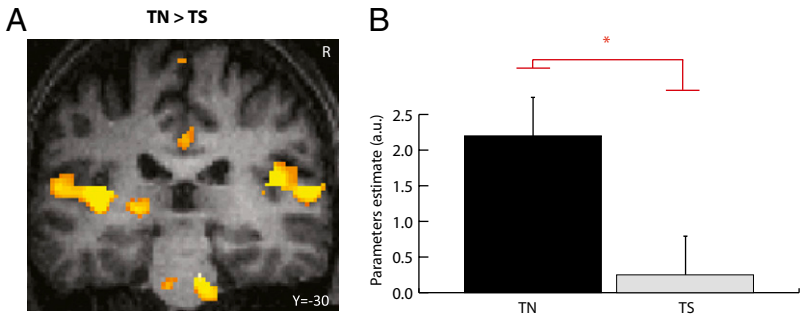

Fig. 3. Difference in responses to TN and TS. (*A*) Brain areas showing significant responses for tones presented during NREM sleep outside spindles (TN) and not to tones presented during spindles (TS). Functional results are displayed on an individual structural image (display at $P < 0.001$, uncorrected). (*B*) Mean parameter estimates (arbitrary units ± SEM) for TN and TS in the right Heschl's gyrus. *$P \leq 0.05$.

followed by an induced K complex. This finding suggests that K complexes triggered by auditory stimulation are associated with a further recruitment of TC loops. In addition, auditory stimulation inducing a K complex resulted in significantly larger responses in the inferior frontal gyrus (Fig. 4*C*). Intriguingly, this area precisely corresponds to the ventral frontal area, which is systematically recruited by spontaneous slow waves during NREM sleep (17). These results echo the stereotypical slow oscillation elicited by transcranial magnetic stimulation delivered over sensorimotor cortex during NREM sleep (26). Our data further suggest that a K complex induced by sensory stimulation is associated with both a response specific to the sensory modality in the corresponding TC circuits and the ignition of a stereotypical response pattern characteristic of the slow oscillation. This induced response arises from the pervasive intrinsic bistability in TC networks and propagates in the brain along preferential trajectories that begin to be identified (17, 27).

In sum, our findings demonstrate the close interplay between spontaneous brain activity and brain responses induced by external stimulation. Not only does spontaneous brain activity, especially sleep spindles, profoundly influence sound processing during NREM sleep, but in turn, auditory stimulation can also trigger a stereotypical response—the activation patterns of which are quite similar to those found during slow oscillation.

Our results show that the brain continues to respond to auditory stimulation during NREM sleep, although much less consistently than during wakefulness, especially during spindles. We stress that the detection of a significant response to sensory stimulation in a particular brain area does not imply that the information is conveyed and decoded as during wakefulness. On the contrary, we surmise that the specific oscillations of NREM sleep, especially the slow oscillation and spindles, shape the neural response to sensory inputs and profoundly modify their decoding.

The functional distortion of external inputs associated with spindles raises the question of which type of information continues to be accurately processed by the brain during spindles. We speculate that endogenous information continues to be processed, possibly in relation to recently encoded experience. Indeed, it has been shown that spindle density increases after declarative (28) and procedural motor learning (29). Although the mechanisms relating spindle activity to memory processing remain elusive, it is known that spike trains reproducing spontaneous spindle discharges are efficient in modifying excitatory neocortical synapses and in inducing long-term potentiation in cortical slices (30). In this view, the neural processes taking place during spindles would allow a functional isolation of brain circuits from incoming stimuli and promote cellular interactions underpinning brain plasticity.

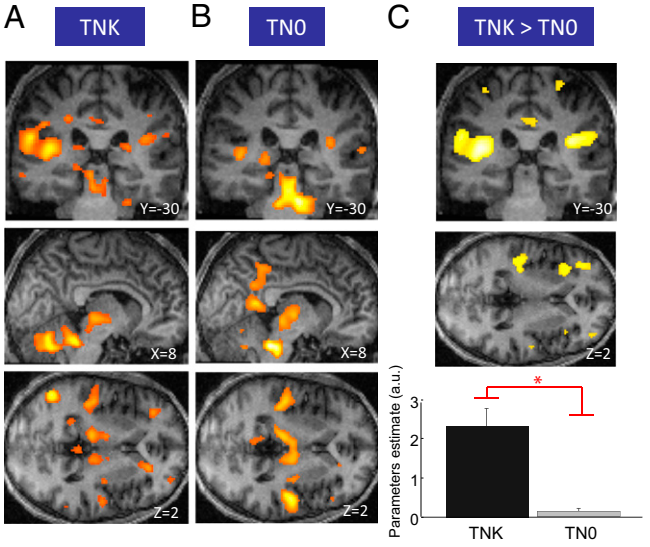

Fig. 4. Brain regions activated in relation to tones during NREM sleep (outside spindles), followed (TNK) or not followed (TN0) by a K complex. (*A*) Significant responses associated with tones presented during S2-3 NREM sleep, in the absence of ongoing spindles, and when tones were followed by a K complex (TNK). (*B*) Significant responses associated with tones presented during S2-3 NREM sleep, in the absence of ongoing spindles, and when tones were not followed by a K complex (TN0). (*C Top and Middle*) Brain areas showing larger activations for TNK compared with TN0. Although responses to both TNK and TN0 overlap with areas recruited by TN, responses to TNK are significantly larger than those to TN0 in the primary auditory cortex and inferior frontal gyrus. (*Bottom*) Mean parameter estimates (arbitrary units ± SEM) for TNK and TN0 in the right Heschl's gyrus. *$P \leq 0.05$. Functional results are displayed on an individual structural image (display at $P < 0.001$, uncorrected) at different levels of the *x*, *y*, and *z* axes as indicated for each section.

Materials and Methods

Population. Nineteen (9 females) healthy, right-handed, young (age range 18–25; mean age 21.30) subjects gave their written informed consent and received financial compensation for their participation in this study, which was approved by the University of Liège Faculty of Medicine Ethics Committee. Participants were free of any history of medical, traumatic, psychiatric, or sleep disorder, as assessed by a semistructured interview. All participants were nonsmokers and moderate caffeine and alcohol consumers. None were on medication. They were not sleep-deprived, as assessed by wrist actigraphy. None of the subjects complained of excessive daytime sleepiness (Epworth Sleepiness Scale; ref. 31) or sleep disturbances (Pittsburgh Sleep Quality Index Questionnaire; ref. 32). All participants had normal scores at the 21-item Beck Anxiety Inventory (33) and the 21-item Beck Depression Inventory II (34). None had worked on night shifts during the last year or traveled through more than one time zone during the last 2 mo.

Extreme morning and evening types, as assessed by the Horne–Ostberg Questionnaire (35), were not included.

Before the experimental night, volunteers followed a 4-d constant sleep schedule, assessed by wrist actigraphy (Actiwatch) and sleep diaries, to ensure that they were not sleep-deprived. Volunteers were asked to refrain from all caffeine- and alcohol-containing beverages and intense physical activity for 3 d before participating in the study. During the experimental night, subjects reported to the laboratory at 9:00 PM. First, actigraphy and sleep diaries were checked for compliance with the sleep schedule. After EEG cap was set up and the quality of the signal was checked within the scanner, fMRI acquisitions were started.

Auditory Stimulation. Pure tones (300 ms, 400 Hz) were presented binaurally by using headphones during the whole scanning session, through high-fidelity, MRI-compatible electrodynamic earmuff headphones with gradient noise suppression (MR Confon). The sound intensity was constant throughout the night and set individually before the experimental session. During this test fMRI session using the same echoplanar sequence, subjects were requested to adjust the sound intensity to a level that was easily perceived above the scanner noise. During the experimental session, sounds were delivered randomly with a 70% probability of occurrence at each scan. This procedure corresponded to the delivery of a sound every 7.044 s on average.

EEG Acquisition and Analysis. EEG was recorded simultaneously with fMRI acquisitions by using two MR-compatible, 32-channel amplifiers (BrainAmp MR Plus; Brain Products) and a MR-compatible EEG cap (BrainCap MR; Falk Minow Services) with 64 ring-type electrodes. EEG caps included 62 scalp channels, as well as one electrooculogram, one chin electromyogram, and one electrocardiogram (ECG) channels. By using abrasive electrode paste (ABRALYT 2000; FMS), electrode–skin impedance was kept at <5 kOhm in addition to the 5-kOhm resistor built into the electrodes. Electrodes were online referenced to FCz. EEG was digitized at 5,000-Hz sampling rate with 500-nV resolution. Data were analog-filtered by a band limiter low-pass filter at 250 Hz (30 dB per octave) and a high-pass filter with 10-s time constant corresponding to a high-pass frequency of 0.0159 Hz. Data were transferred outside the scanner room through fiber-optic cables to a personal computer where the EEG system running Vision Recorder software (v1.03; Brain Products) was synchronized to the scanner clock. Sleep EEG was monitored online with RecView software (Brain Products).

For analysis, EEG data were low-pass filtered [finite impulse response (FIR) filter; −36 dB at 70 Hz], down-sampled to 250 Hz, and rereferenced to the averaged mastoids. Scanner gradient artifacts were removed in Vision Analyzer by using an adaptive average subtraction (36). Pulse-related artifacts were removed by using an algorithm based on independent component analysis (37). Sleep staging followed standard criteria (38) and identified periods of S2 and S3 sleep, free of any artifact, arousal, or shifts in vigilance states, during which the EEG and fMRI data were analyzed. On average (±SD), subjects spent 36.4 (16.4) min in S2, 13.3 (10.8) min in S3, and 14 (10.2) min in S4 of NREM sleep. Combined S2, S3, and S4 represented 79.7% (9.3%) of time in the scanner for the sleep acquisition. Only stable S2-3 epochs lasting >5 min were considered.

In these epochs, sleep spindles were identified and slow wave activity was computed because they were to be included in the fMRI analysis. Sleep spindles were automatically detected on Fz, Cz, and Pz by using an algorithm adapted from Mölle and colleagues (16). For spindle detection, data were bandpass-filtered between 11 and 15 Hz by using linear-phase FIR filters (−3 dB at 11.1 and 14.9 Hz). The root mean square of the filtered signal was calculated by using a time window of 0.25 s. Spindles were identified by thresholding the spindle root mean square signal at its 95th percentile. Slow-wave activity was computed as the square root of the energy of the signal in the 0.5–4-Hz frequency band averaged over each repetition time.

Induced K complexes were also automatically identified in these selected epochs by using a method similar to that used for the detection of slow waves (17). Only those slow waves with a peak-to-peak amplitude of >75 μV, a duration of >500 ms (38), and a maximal negativity occurring within a period of 100–800 ms after the tone onset were considered as K complexes evoked by the delivered tones, and they were further used for subcategorization of tones during NREM sleep outside spindles.

Processing of ERPs was conducted for completeness, although the data acquisition was geared toward fMRI analysis rather than ERP characterization. In particular, the number of TS trials was expectedly too small to provide optimal ERP quality. EEG was analyzed by using SPM EEG (SPM5; http://www.fil.ion.ucl.ac.uk/spm/software/spm5/) implemented in MATLAB [Version 7.7 (R2008b); MathWorks]. After artifact correction and rereferencing to the averaged mastoids, the EEG recordings were bandpass-filtered (0.5–20 Hz). In each subject, trials corresponding to the different types of tones (TW, TN, TS) were then extracted by epoching the EEG on Cz channel from 100 ms before to 400 ms after each stimulus onset. The mean (SD) number of trials per subject for TW, TN, and TS was, respectively, 161.3 (96.5), 534.3 (198.8), and 30 (11.2). Each trial was visually checked to reject those in which the EEG was >150 μV. Averages were then computed for each tone category in each subject. Amplitudes of N1 and P2 components were tested across subjects by using ANOVA with tone category as within-subject factor. For each trial, the N1 amplitude was defined as the maximal negativity between 75 and 125 ms after stimulus onset and the P2 amplitude as the maximal positivity between 175 and 250 ms after stimulus onset (39). For display, the mean averages of ERPs were also averaged across subjects (Fig. S2).

fMRI Data Acquisition and Analysis. Multislice, T2*-weighted fMRI images were obtained by using a 3-tesla MR scanner (Allegra; Siemens), with a gradient echo-planar sequence using axial slice orientation and reduced slew rate for efficient gradient artifact rejection and reduced acoustic noise (32 slices; voxel size: 3.4 × 3.4 × 3 mm^3; matrix size: 64 × 64 × 32; TR = 2,460 ms; TE = 40 ms; flip angle = 90°; delay = 0). Subjects were asked to relax and try to sleep in the scanner during the first half of the night starting at around midnight, during which fMRI and EEG data were acquired continuously. It was mentioned that tones would be presented during the session, but the participants were instructed not to pay attention to these stimuli. To avoid movement-related EEG artifacts, each subject's head was immobilized in the head coil by a vacuum pad. Subjects stayed until they indicated by button press that they would like to go out or for a maximum of 4,600 scans (~189 min). The number of acquired scans varied between 1,195 and 4,599 [3,401 ± 965 scans or 139 min ± 40 min (mean ± SD)]. A structural T1-weighted 3D magnetization-prepared rapid acquisition gradient-echo sequence (TR = 1,960 ms; TE = 4.43 ms; inversion time = 1,100 ms; field of view = 230 × 173 mm^2; matrix size = 256 × 192 × 176; voxel size = 0.9 × 0.9 × 0.9 mm^3) was also acquired in all subjects.

Functional volumes were analyzed by using Statistical Parametric Mapping 5 (SPM5; http://www.fil.ion.ucl.ac.uk/spm/software/spm5/) implemented in MATLAB (Version 7.7 (R2008b); MathWorks). The series of consecutive fMRI volumes corresponding to selected S2-3 or wake periods were selected from the complete fMRI time series and constituted a session (Fig. 1*B*). fMRI time series were corrected for head motion, spatially normalized (voxel size = 2 × 2 × 2 mm^3; resampled using spline interpolation) to an echo planar imaging template conforming to the Montreal Neurological Institute space, and spatially smoothed with a Gaussian kernel of 8-mm FWHM. The analysis of fMRI data, based on a mixed effects model, was conducted in two serial steps, accounting, respectively, for intraindividual (fixed effects) and interindividual (random effects) variance.

Within these sessions, the statistical analysis of fMRI data was aimed at characterizing the brain responses to various categories of tones, according to their occurrence outside (TN) or within (TS) detected spindles. A tone was classified in the TS category if its onset occurred within the bounds of a detected spindle. TN were further classified into two subcategories according to whether (TNK) or not (TN0) they were followed by an evoked K complex (for the tone to be classified as TNK, the maximal negativity had to occur within a period of 100–800 ms after the tone onset). There were, on average, 46 TNK and 488 TN0 per subject. In addition, tones that were presented during periods of wakefulness prior to and after sleep emergence during the scanning session were considered for a separate analysis (TW).

For each subject, the vectors including TN (TNK and TN0) and TS onsets were convolved with the three canonical basis functions (hemodynamic response function and its derivative and dispersion) and used as regressors in the individual design matrix. Regressors containing the spindle onsets and slow wave activity, convolved with the three basis functions, were also included as variables of no interest, because we aimed at identifying the sound-related activations over and above these spontaneous brain activities of NREM sleep. Waking sessions were analyzed separately: The vectors including TW onsets were convolved with the three canonical basis functions and used as regressors. To take into account the artifacts related to cardiac cycle, an estimation of R–R intervals derived from ECG was included as a regressor of no interest in all individual design matrices. Movement parameters estimated during realignment (translations in *x*, *y*, and *z* directions and rotations around *x*, *y*, and *z* axes) and a constant vector were also included in the matrix as regressors of no interest. High-pass filtering was implemented in the matrix design by using a cutoff period of 128 s to remove low-frequency drifts from the time series. Serial correlations in fMRI signal were estimated by using an autoregressive (order 1) plus white noise model and a restricted maximum-likelihood algorithm. The main effects of the TN, TS, TW, TNK,

and TN0 were then tested by a linear contrast, generating statistical parametric maps. These individual contrast images were further smoothed (6-mm FWHM Gaussian kernel) and entered in a second-level analysis. The second-level analysis consisted of ANOVA with the basis set (three levels) as factor. The error covariance was not assumed to be independent between regressors, and a correction for nonsphericity was applied. The resulting set of voxel values constituted maps of F statistics [SPM(F)]. To correct for multiple comparisons, statistical inferences were reported in regions of interest previously identified in neuroimaging studies of NREM sleep or auditory tasks (Tables S1, S2, and S3) by using spherical volumes (10-mm sphere radius; i.e., ~4,000 mm^3; small volume correction), and a threshold of $P < 0.05$ corrected. Results obtained from SPM analysis of fMRI data only revealed brain areas that systematically increase their BOLD signal in relation to TN, TS, TW, TNK, and TN0 and compared with the spontaneous brain activity of NREM sleep (spindles, slow waves) and the baseline activity. In S2-3 sessions, this baseline mainly consisted of activity that was not accounted for by spindles and slow waves (e.g., EEG activity at >4 Hz and not in the spindle frequency range). Note that responses to tones during wakefulness and sleep could not be directly compared because their baseline activities were different. For the comparison between TN and TS, an exclusive mask at a lenient threshold ($P < 0.5$) was applied at the second level to demonstrate the activations related to TN that were not accounted for by TS. Furthermore, parameter estimates corresponding to the respective effects of TN and TS in the right Heschl's gyrus (58, −14, 6) were compared across subjects by using ANOVA with tone category as within-subject factor. For this comparison, coordinates of the right Heschl's gyrus were derived from the peak voxel in this area during wakefulness (TW). TNK and TN0 were similarly compared.

ACKNOWLEDGMENTS. This work was supported by the Belgian Fonds National de la Recherche Scientifique (FNRS), Fondation Médicale Reine Elisabeth, Research Fund of the University of Liège, and "Interuniversity Attraction Poles Programme—Belgian State—Belgian Science Policy". T.T.D.-V., M. Boly, M.D., E.B., C.P., and P.M. are supported by the FNRS. T.T.D.-V. was also supported by a European Sleep Research Society Grant, the Belgian American Educational Foundation, the Belgian Neurological Society, Fonds Léon Frédéricq, the Horlait– Dapsens Medical Foundation, and Wallonie–Bruxelles International. M.S. was supported by Austrian Science Fund Erwin Schrödinger Fellowship J2470-B02. M. Bonjean and T.J.S. were supported by the Howard Hughes Medical Institute, National Institutes of Health Grant R01 EB009282, and Fonds Léon Frédéricq (Belgium).

1. Hobson JA (2005) Sleep is of the brain, by the brain and for the brain. *Nature* 437: 1254–1256.
2. Edeline JM, Manunta Y, Hennevin E (2000) Auditory thalamus neurons during sleep: Changes in frequency selectivity, threshold, and receptive field size. *J Neurophysiol* 84:934–952.
3. Edeline JM (2003) The thalamo-cortical auditory receptive fields: Regulation by the states of vigilance, learning and the neuromodulatory systems. *Exp Brain Res* 153: 554–572.
4. Bastuji H, García-Larrea L (1999) Evoked potentials as a tool for the investigation of human sleep. *Sleep Med Rev* 3:23–45.
5. Portas CM, et al. (2000) Auditory processing across the sleep-wake cycle: Simultaneous EEG and fMRI monitoring in humans. *Neuron* 28:991–999.
6. Steriade M, McCormick DA, Sejnowski TJ (1993) Thalamocortical oscillations in the sleeping and aroused brain. *Science* 262:679–685.
7. Steriade M, McCarley RW (1990) *Brainstem Control of Wakefulness and Sleep* (Plenum Press, New York).
8. De Gennaro L, Ferrara M (2003) Sleep spindles: An overview. *Sleep Med Rev* 7: 423–440.
9. Steriade M, Domich L, Oakson G, Deschênes M (1987) The deafferented reticular thalamic nucleus generates spindle rhythmicity. *J Neurophysiol* 57:260–273.
10. Steriade M (1995) Thalamic origin of sleep spindles: Morison and Bassett (1945). *J Neurophysiol* 73:921–922.
11. Steriade M, Jones E, Llinas R (1990) *Thalamic Oscillations and Signaling* (Wiley-Interscience, New York).
12. Contreras D, Steriade M (1996) Spindle oscillation in cats: the role of corticothalamic feedback in a thalamically generated rhythm. *J Physiol* 490:159–179.
13. Steriade M (1991) *Normal and Altered States of Function,* Cerebral Cortex, eds Peters A, Jones EJ (Plenum, New York), Vol 9, pp 279–357.
14. Cote KA, Epps TM, Campbell KB (2000) The role of the spindle in human information processing of high-intensity stimuli during sleep. *J Sleep Res* 9:19–26.
15. Elton M, et al. (1997) Event-related potentials to tones in the absence and presence of sleep spindles. *J Sleep Res* 6:78–83.
16. Mölle M, Marshall L, Gais S, Born J (2002) Grouping of spindle activity during slow oscillations in human non-rapid eye movement sleep. *J Neurosci* 22:10941–10947.
17. Dang-Vu TT, et al. (2008) Spontaneous neural activity during human slow wave sleep. *Proc Natl Acad Sci USA* 105:15160–15165.
18. Schabus M, et al. (2007) Hemodynamic cerebral correlates of sleep spindles during human non-rapid eye movement sleep. *Proc Natl Acad Sci USA* 104:13164–13169.
19. Holcomb HH, et al. (1998) Cerebral blood flow relationships associated with a difficult tone recognition task in trained normal volunteers. *Cereb Cortex* 8:534–542.
20. Gaab N, Gaser C, Zaehle T, Jancke L, Schlaug G (2003) Functional anatomy of pitch memory—an fMRI study with sparse temporal sampling. *Neuroimage* 19:1417–1426.
21. Velluti RA (2007) *The Auditory System in Sleep* (Academic, New York).
22. Rosanova M, Timofeev I (2005) Neuronal mechanisms mediating the variability of somatosensory evoked potentials during sleep oscillations in cats. *J Physiol* 562: 569–582.
23. McCormick DA, Feeser HR (1990) Functional implications of burst firing and single spike activity in lateral geniculate relay neurons. *Neuroscience* 39:103–113.
24. Sherman SM, Guillery RW (2002) The role of the thalamus in the flow of information to the cortex. *Philos Trans R Soc Lond B Biol Sci* 357:1695–1708.
25. Steriade M (2006) Grouping of brain rhythms in corticothalamic systems. *Neuroscience* 137:1087–1106.
26. Massimini M, et al. (2007) Triggering sleep slow waves by transcranial magnetic stimulation. *Proc Natl Acad Sci USA* 104:8496–8501.
27. Murphy M, et al. (2009) Source modeling sleep slow waves. *Proc Natl Acad Sci USA* 106:1608–1613.
28. Schabus M, et al. (2004) Sleep spindles and their significance for declarative memory consolidation. *Sleep* 27:1479–1485.
29. Morin A, et al. (2008) Motor sequence learning increases sleep spindles and fast frequencies in post-training sleep. *Sleep* 31:1149–1156.
30. Rosanova M, Ulrich D (2005) Pattern-specific associative long-term potentiation induced by a sleep spindle-related spike train. *J Neurosci* 25:9398–9405.
31. Johns MW (1991) A new method for measuring daytime sleepiness: The Epworth sleepiness scale. *Sleep* 14:540–545.
32. Buysse DJ, Reynolds, CF, 3rd, Monk TH, Berman SR, Kupfer DJ (1989) The Pittsburgh Sleep Quality Index: A new instrument for psychiatric practice and research. *Psychiatry Res* 28:193–213.
33. Beck AT, Epstein N, Brown G, Steer RA (1988) An inventory for measuring clinical anxiety: Psychometric properties. *J Consult Clin Psychol* 56:893–897.
34. Steer RA, Ball R, Ranieri WF, Beck AT (1997) Further evidence for the construct validity of the Beck depression Inventory-II with psychiatric outpatients. *Psychol Rep* 80: 443–446.
35. Horne JA, Ostberg O (1976) A self-assessment questionnaire to determine morningness-eveningness in human circadian rhythms. *Int J Chronobiol* 4:97–110.
36. Allen PJ, Josephs O, Turner R (2000) A method for removing imaging artifact from continuous EEG recorded during functional MRI. *Neuroimage* 12:230–239.
37. Srivastava G, Crottaz-Herbette S, Lau KM, Glover GH, Menon V (2005) ICA-based procedures for removing ballistocardiogram artifacts from EEG data acquired in the MRI scanner. *Neuroimage* 24:50–60.
38. Rechtschaffen A, Kales A (1968) *A Manual of Standardized Terminology, Techniques and Scoring System for Sleep Stages of Human Subjects* (Brain Information Service/Brain Research Institute, University of California, Los Angeles).
39. Colrain IM, Campbell KB (2007) The use of evoked potentials in sleep research. *Sleep Med Rev* 11:277–293.